Automatic migration velocity analysis and multiples

Wim A. Mulder, Shell International Exploration & Production*
Tristan van Leeuwen, Delft University of Technology

SUMMARY

Migration velocity analysis attempts to find a velocity model by focusing a migration image with respect to a redundant coordinate, here a shift at depth between forward and time-reversed wavefields. An automatic algorithm requires a wave propagation algorithm and an optimization scheme. A 2D frequency-domain finite-difference code for the two-way wave equation provides the wavefields. A gradient-based minimization scheme should find the velocity model best focuses the migration image. In the presence of multiples, the method may provide incorrect results because there is no mechanism to distinguish between primary and multiple reflections. Two modifications are proposed that may improve the result in the presence of multiples.

INTRODUCTION

Full waveform inversion based on least-squares fitting of modeled to observed data requires an initial model that explains the observed data within less than half a wavelength. Otherwise, a gradient-based minimization scheme will converge to a nearby local minimum, leading to the wrong model. Several authors have come up with partial solutions to this problem. Diving wave tomography (Pratt et al., 1996) reconstructs the velocity by using transmitted events but is limited to the maximum depth reached by diving waves. Migration-Based Traveltime Tomography (Clément et al., 2001) demigrates the migrated data and compares the result to the observed data, thereby enlarging the domain of starting models that lead to convergence to the global minimum. Because the basic driving mechanism is stacking, the initial velocity model should be good enough to provide some energy in the migration image for the primary reflections. Differential Semblance Optimization (DSO) (Symes and Kern, 1992) tries to flatten common image gathers in the migrated domain by minimizing differences of neighboring migrated traces. Shen et al. (2003) introduced a focusing optimization based on shifts in depth or subsurface offset as a redundant coordinate rather than shot position or offset, using the double square-root wave equation as wave propagator. Examples for the two-way wave equation, employing a 2D frequency-domain finite-difference code for the constant-density acoustic wave equation, show that the approach has problems with multiples in the data (Mulder, 2008).

We propose two algorithmic modifications that may reduce the adverse effect of multiples on the velocity model obtained by migration velocity analysis. The first introduces a bias towards the higher velocities, the second involves the difference between modelled and observed data.

METHOD

The velocity analysis technique focuses a migration image in terms of a shift at depth rather than surface offset (MacKay and Abma, 1992; Shen et al., 2003; Symes et al., 2004; Stolk and de Hoop, 2006). If p_s denotes the wave field due to a shot indexed by s in the frequency domain at an angular frequency ω and $q_{r(s)}$ is the time-reversed wave field generated by the recorded data for that shot at receivers indexed by $r(s)$, the usual migration image or reflectivity is proportional to

$$\rho(x,z) = \sum_{s,r(s),\omega} \omega^2 p_s^*(x,z,\omega) q_{r(s)}(x,z,\omega). \qquad (1)$$

Because our examples will be 2D, we have specialized to x and z. We obtain a generalized reflectivity by introducing a horizontal shift h_x and/or vertical shift h_z of the two wave fields before correlation:

$$R(x,z;h_x,h_z) = \sum_{s,r(s),\omega} \omega^2 p_s^*(x-h_x,z-h_z,\omega) q_s(x,z,\omega).$$

This expression is convenient from a computational point of view. For diagnostics, $R(x+h_x/2,z+h_z/2;h_x,h_z)$ is more suitable. A focusing functional is

$$J_x^{\mathrm{F}} = \frac{\frac{1}{2}\sum_{x,z,h_x} W(x,z) w^2(h_x) |\Xi_x R(x,z;h_x,0)|^2}{\frac{1}{2}\sum_{x,z,h_x} W(x,z) |R(x,z;0,0)|^2}. \qquad (2)$$

The operator Ξ_x represents a spatial filter that removes steeply dipping events by the application of a 2D fast Fourier transform in x and z, multiplication by $\sqrt{k_z^2/(k_x^2+k_z^2)}$, and an inverse FFT. Here k_x and k_z are the wave numbers in the x- and z-direction, respectively. An additional weighting function $W(x,z)$ is included to, for instance, boost the deeper reflectors. The normalization by $R(x,z;0)$ avoids unwanted behaviour such as selection of a velocity that moves all reflectors outside the computational domain. The function $w(h_x)$ should penalize contributions at non-zero shift h_x. A simple choice is $w(h_x) = h_x$. Minimization of J_x^{F} should concentrate the energy around $h_x = 0$ and provide the best velocity model. Note, however, that the data used for computing the generalised reflectivity should contain primary reflections only, which is a severe restriction. We can define a similar functional J_z^{F} for a shift h_z in the z-direction and a filter Ξ_z that employs $\sqrt{k_x^2/(k_x^2+k_z^2)}$. This is required for the focusing of steeply dipping reflectors. In general, the sum $J_x^{\mathrm{F}} + J_z^{\mathrm{F}}$ should be minimized. Here, we will only consider J_x^{F}. An additional spatial low-cut filter can be applied to remove smooth patterns in the reflectivity due to diving waves and refractions, as proposed earlier (Mulder and Plessix, 2004). We performed the minimization with the L-BFGS method (Byrd et al., 1995). This requires the gradient of the functional with respect to the velocity model parameters which can be derived in a straight-forward manner by means of the adjoint-state method. Examples can be found elsewhere (Mulder, 2008).

MULTIPLES

Bias

Asymptotic analysis provides some insight in how multiples may lead to the wrong velocity model. If we describe wave propagation with the convolutional model and NMO (normal move-out) velocities $v_{\rm nmo}(t_0)$, the asymptotic analysis shows that non-focused events appear as hyperbolas as a function of two-way traveltime t_0 and the offset-at-depth h_x (van Leeuwen and Mulder, 2007, 2008). Note that depth is replaced by two-way traveltime in this type of modeling. The asymptotic analysis leads to the relation

$$h_x = h\left[1-(v_{\rm nmo}/\bar{v}_{\rm nmo})^2\right] \tag{3}$$

(van Leeuwen and Mulder, 2008). Here h is surface offset and $\bar{v}_{\rm nmo}$ denotes the true model. The asymptotic analysis shows that the closer the model approaches to true one, the narrower the hyperbola becomes (the smaller the range of h_x, given $h_{\rm min} \le h \le h_{\rm max}$), until the hyperbola degenerates into a single point for the true model. Equation 3 also teaches us that for a one-sided acquisition, say with positive surface offsets ($h > 0$), the energy on the hyperbolas will be reside mainly at negative or positive values of the offset-at-depth h_x, depending on whether the velocity is smaller or higher than the true one.

Figure 1 illustrates what happens in the presence of multiples. For NMO velocities smaller than the true ones, the energy is concentrated at positive values of the shift h_x (second panel from the left), for the exact model, the primaries focus at zero h_x, whereas the energy of the multiples resides at the negative values of h_x. The artifacts, visible for instance at positive h_x in the correct velocity model, are caused by the finite range of frequencies and the finite aperture of the acquisition. The rightmost panel corresponds to a velocity that is too high. Now both primaries and multiples have most of there energy positioned at negative values of h_x.

In a typical marine situation, the free-surface have seen a lower effective velocity than the primary reflections. We can exploit this fact by introducing a bias b in the weighting function that penalizes offset shift: $w(h_x) = \min(0,h_x) + b\max(0,h_x)$. For an acquisition with positive surface offsets, $b > 1$ favors higher velocities. This is similar to the filter introduced by Mulder and ten Kroode (2002) for ray-based DSO and further developed by Li and Symes (2007) for NMO-based DSO.

We can design a more sophisticated weighting function $w(h_x)$ to account for the width of the Fresnel zone in finite-frequency data, but have not used that one here.

Data difference

Because it is nearly impossible to construct a background model that does not produce any back-scatter with the full wave equation, the following variant may help. The idea is to migrate the difference between synthetic and observed data instead of the observed data themselves. This will cancel multiples if they are properly modelled. The wave operator for constant-density acoustics in the frequency domain is $L = -(\omega/c)^2 - \Delta$. The forward problem $Lp = f$ with source function f provides synthetic data Sp at the receivers, where S is sampling or interpolation operator that maps the wavefield in the computational domain to the receiver position. The corresponding time-reversed wavefield q obeys $L^{\rm H}q_1 = S^{\rm T}(Sp - p^{\rm obs})$, where the superscript $^{\rm T}$ denotes the transpose and $^{\rm H}$ the conjugate transpose. Also, the time-reversed wavefield q_0 is obtained from the observed data $p^{\rm obs}$ by $L^{\rm H}q_0 = -S^{\rm T}p^{\rm obs}$, which is the same as used for the previous functional $J_x^{\rm F}$. As before, generalised reflectivities for each shot and frequency can be defined as

$$\rho_{k,s,\omega}(\mathbf{x},\mathbf{h}) = \sum_{r(s)} \omega^2 p^*_{s,\omega}(\mathbf{x}-\mathbf{h}) q_{k,r(s),\omega}(\mathbf{x}),$$

for $k = 0$ and 1, leading to $R_k(\mathbf{x},\mathbf{h}) = \sum_{s,\omega}\rho_{k,s,\omega}(\mathbf{x},\mathbf{h})$. A focusing functional is

$$J_x^{\rm D} = \frac{\frac{1}{2}\sum_{\mathbf{x},h_x} W(\mathbf{x})w^2(h_x)|\Xi_x R_1(\mathbf{x},\mathbf{h})|^2}{\frac{1}{2}\sum_{\mathbf{x},h_x} W(\mathbf{x})|R_0(\mathbf{x},0)|^2}, \tag{4}$$

for $\mathbf{h} = (h_x, 0)$. A similar definition can be given for $J_z^{\rm D}$. The penalization weight is now $w(h) = w_0 + |h|$ with $w_0 \ge 0$. Note that the source wavelet should be known to get a proper subtraction of modelled and observed data. For real data, it will be better to drop the constant-density assumption and use an acoustic or perhaps even an elastic propagator.

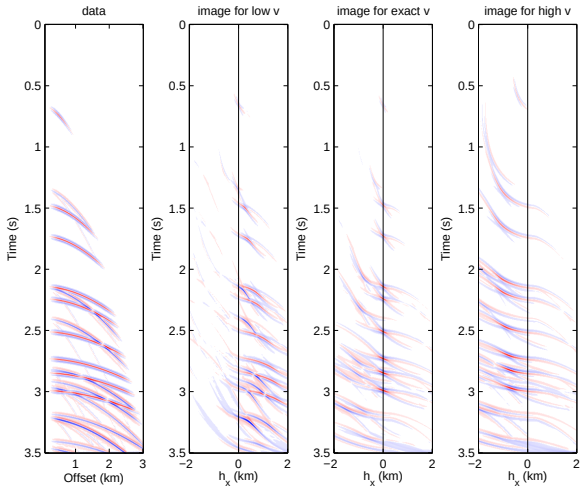

Figure 1: The left panel shows data generated with the convolutional model including first-order free-surface multiples generated by convolving the data with themselves. The other panels display the generalized images, where time now parametrized depth. From left to right, the NMO velocity is too low, exact, or too high.

EXAMPLES

We generated synthetic data with a time-domain code for the 2D constant-density acoustic wave equation, using the model shown in figure 2 and placing 49 shots with a 50 m spacing between $x = -200$ and 2,200 m at 5 m depth and receivers with 25 m spacing between offsets of 50 and 2,000 m at the

same depth as the source. For the numerical inversion experiments, we employed a fourth-order frequency-domain code with a grid spacing of 10 m and selected frequencies between 12 and 22 Hz at a 0.5 Hz interval.

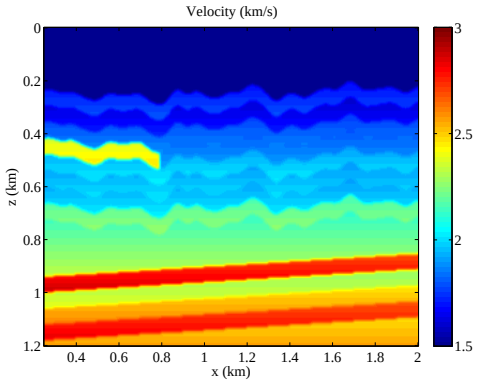

Figure 2: Central part of the true velocity model.

After removal of the direct wave by simple blanking, the data with multiples led to the reconstructed velocity model shown in figure 3. The iterations were started by first finding a optimal velocity model that increased linearly with depth, using a one-parameter search algorithm, and then proceeding with the L-BFGS minimization method. We stopped after 50 iterations.

A bias $b = 1.2$ produces the results shown in figure 4. The reconstructed velocity model in panel (a) has improved over the one in figure 3. In panel (b), we observe a slight increase of the velocity in the shallower part of the domain. The section in figure 3c at $x = 1$ km shows the focussing around $h_x = 0$ km, with peaks slightly shifted towards the negative values of h_x because of the bias. We also note a rather strong overshoot and phase error at the strong reflector around 0.9 km depth in figure 3b. This appears to be a flaw of the method caused by the scaling with $\frac{1}{2}\sum_{x,z,h_x} W(x,z)|R(x,z;0,0)|^2$ in the functional J_x^{F}. If we remove this scaling and just take the numerator of J_x^{F}, the method will not converge to a reasonable model when we perform the search for the best linear velocity model. If we include it, the method tends to create large over- or undershoots in the velocity model at strong reflectors. These have the effect of compressing the migrated energy in the depth direction, thereby reducing the size of the numerator of J_x^{F} while increasing the denominator at the same time. We have not yet found a cure for this problem, other than stopping the iterations after a fixed count.

The alternative functional J_x^{D} provided the results shown in figure 5 after 25 iterations. No preprocessing of the data was applied. Apparently, the reflectors are now reconstructed as a part of the velocity model. The functional J_x^{D} also tends to produce large velocity over- or undershoots around strong reflectors, just as J_x^{F} did.

With both method, the number of iterations required to get a reasonable velocity model is far smaller than with least-squares minimization, which tends to take hundreds of iterations (Mulder et al., 2006).

DISCUSSION AND CONCLUSIONS

Migration velocity analysis may provide an incorrect velocity model in the presence of multiples. We have proposed two variants and tested them with a two-way propagator. One has a bias towards higher velocities, the other incorporates the difference between synthetic and observed data.

Note that there is a fundamental difference between the two methods. The first one assumes the presence of only primary reflections. The resulting velocity model should be kinematically correct if the data obey this assumption. The reconstructed model may serve as input for further least-squares fitting in a linearized or nonlinear way (Østmo et al., 2002; Mulder and Plessix, 2004). The bias helps to reduce the effect of multiples if they correspond to events that have seen a lower effective velocity, which is true for surface related multiples. The second method incorporates a data difference and not only provides a background velocity model but also tries to construct the reflectors. Again, this model may be used as input for further least-squares fitting.

The second method provided a somewhat better reconstruction for our simple synthetic data example. Its application to real data will require a fully acoustic or perhaps even elastic generalization of our constant-density method.

ACKNOWLEDGEMENTS

Tristan van Leeuwen carried out his work as part of the research programme of the 'Stichting voor Fundamenteel Onderzoek der Materie (FOM)', which is financially supported by the 'Nederlandse Organisatie voor Wetenschappelijk Onderzoek (NWO)'.

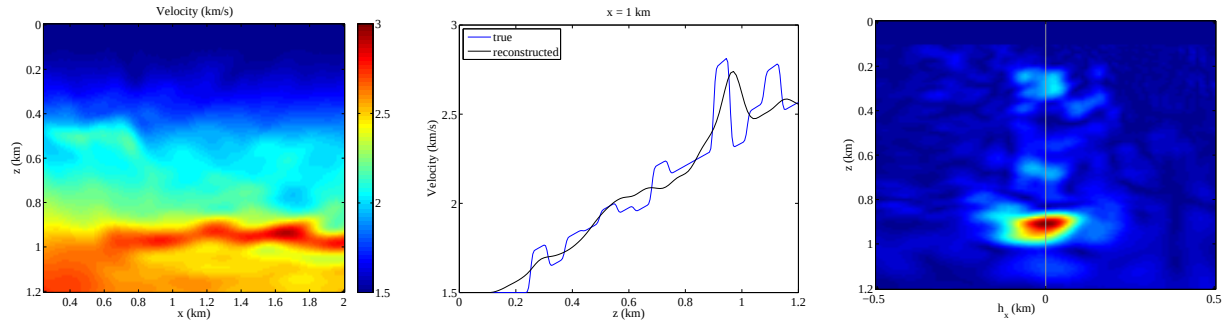

(a) (b) (c)

Figure 3: (a) Reconstructed model using the functional J_x^{F} without bias, (b) vertical cross section, and (c) $|\Xi_x R(x+h_x/2,z;h_x,0)|$ at $x=1\,\mathrm{km}$. The energy should focus around $h_x=0\,\mathrm{km}$.

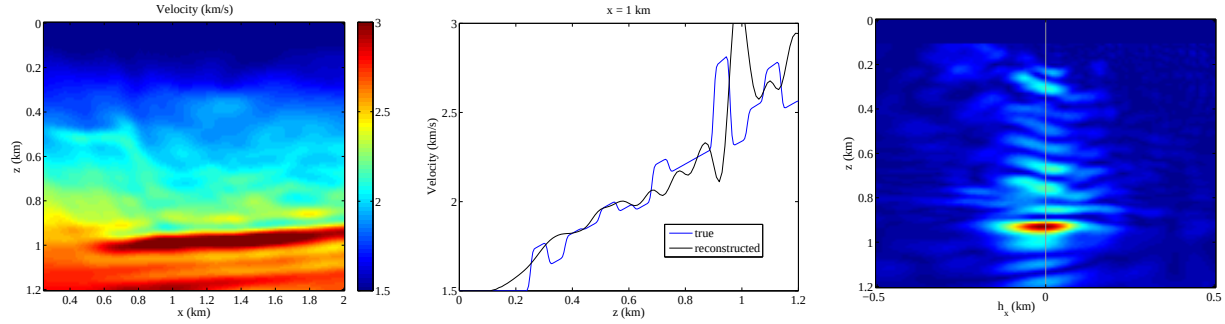

(a) (b) (c)

Figure 4: (a) Reconstructed model using the functional J_x^{F} with a bias of 1.2, (b) vertical cross section, and (c) $|\Xi_x R(x+h_x/2,z;h_x,0)|$ at $x=1\,\mathrm{km}$. The energy should focus slightly to the left of $h_x=0\,\mathrm{km}$ because of the bias.

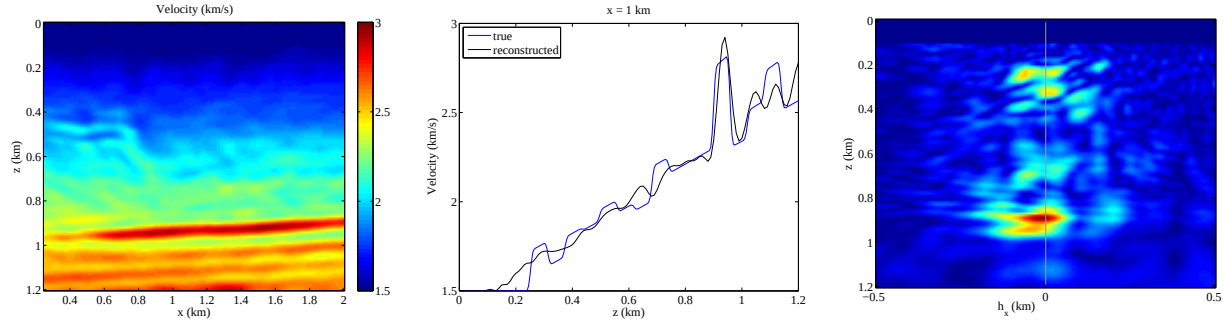

(a) (b) (c)

Figure 5: (a) Reconstructed model using the functional J_x^{D}, (b) vertical cross section, and (c) $|\Xi_x R(x+h_x/2,z;h_x,0)|$ at $x=1\,\mathrm{km}$.

EDITED REFERENCES

Note: This reference list is a copy-edited version of the reference list submitted by the author. Reference lists for the 2008 SEG Technical Program Expanded Abstracts have been copy edited so that references provided with the online metadata for each paper will achieve a high degree of linking to cited sources that appear on the Web.

REFERENCES

Byrd, R. H., P. Lu, J. Nocedal, and C. Zhu, 1995, A limited memory algorithm for bound constrained optimization: SIAM Journal on Scientific Computing, **16**, 1190–1208.

Clément, F., G. Chavent, and S. Gomez, 2001, Migration-based traveltime waveform inversion of 2D simple structures: A synthetic example: Geophysics, **66**, 845–860.

Li, J., and W. W. Symes, 2007, Interval velocity estimation via NMO-based differential semblance: Geophysics, **72**, U75–U88.

MacKay, S., and R. Abma, 1992, Imaging and velocity analysis with depth-focusing analysis: Geophysics, **57**, 1608–1622.

Mulder, W. A., 2008, Automatic velocity analysis with the two-way wave equation: Presented at the 70th Annual International Conference and Exhibition, EAGE.

Mulder, W. A., and R.-E. Plessix, 2004, A comparison between one-way and two-way wave-equation migration: Geophysics, **69**, 149–1504.

Mulder, W. A., R. H. Steenweg, and C. Roos, 2006, Nesterov's method and L-BFGS minimization applied to acoustic migration: Presented at the 68th Annual International Conference and Exhibition, EAGE.

Mulder, W. A., and A. P. E. ten Kroode, 2002, Automatic velocity analysis by differential semblance optimization: Geophysics, **67**, 1184–1191.

Østmo, S., W. A. Mulder, and R. Plessix, 2002, Finite-difference iterative migration by linearized waveform inversion in the frequency domain: 72nd Annual International Meeting, SEG, Expanded Abstracts, 1384–1387.

Pratt, R. G., Z.-M. Song, P. Williamson, and M. Warner, 1996, Two-dimensional velocity models from wide-angle seismic data by wavefield inversion: Geophysical Journal International, **124**, 323–340.

Shen, P., W. W. Symes, and C. C. Stolk, 2003, Differential semblance velocity analysis by wave-equation migration: 73rd Annual International Meeting, SEG, Expanded Abstracts, 2132–2135.

Stolk, C. C., and M. de Hoop, 2006, Seismic inverse scattering in the downward continuation approach: Wave Motion, **43**, 579–598.

Symes, W. W., and M. Kern, 1992, Velocity inversion by differential semblance optimization for 2D common source data: 62nd Annual International Meeting, SEG, Expanded Abstracts, 1210–1213.

Symes, W. W., C. C. Stolk, B. Biondi, and F. Gao, 2004, Reverse time shot-geophone migration: http://www.trip.caam.rice.edu/txt/trip04/papers/twoway.pdf.

van Leeuwen, T., and W. A. Mulder, 2007, Data correlation for velocity inversion: 77th Annual International Meeting, SEG, Expanded Abstracts, 1800–1804.

———2008, Asymptotic comparison of velocity analysis in the image and data domain for layered models: Geophysics, submitted.